THE ASTROPHYSICAL JOURNAL, **260**:124–127, 1982 September 1

DIFFUSE INTERSTELLAR CLOUDS ASSOCIATED WITH DARK CLOUDS

S. R. FEDERMAN
Department of Astronomy, University of Texas at Austin
AND
R. F. WILLSON
Department of Physics, Tufts University
Received 1982 January 11; accepted 1982 March 15

ABSTRACT

Measurements of CH emission at 9 cm toward the bright stars α Cam and κ Cas and from dark clouds near the stars reveal an association between diffuse clouds and dark clouds. Here the term *diffuse clouds* refers to clouds seen in optical absorption; the term *dark clouds* refers to opaque regions on the Palomar Sky Survey observed through radio techniques. The radio emission toward α Cam, and possible emission toward κ Cas, occurs at the same velocity as the optical CH absorption. The column densities derived from both techniques are similar. A dark cloud near each star also shows emission at the velocity of absorption. The column density of CH is larger in the dark cloud. From these data, it is concluded that for most lines of sight, diffuse clouds are the outer, relatively transparent portions of dark clouds.

Subject headings: interstellar: matter — interstellar: molecules — nebulae: general

I. INTRODUCTION

Much of the spectroscopic work on interstellar clouds at optical and radio wavelengths regards the lines detected in the two wavelength bands as coming from distinct objects. Optical absorption occurs in so-called diffuse clouds where visible and ultraviolet radiation can penetrate; radio emission comes from so-called dark clouds, which appear opaque on POSS plates. (For the remainder of the report, these definitions for the two main types of clouds will be used.) The idea of two distinct types of clouds may be too simplistic—in particular, for studies of the molecular chemistry of interstellar clouds. For a few clouds, both optical absorption and radio emission are seen. Toward ζ Oph, Crutcher (1979), Liszt (1979), and Willson (1981) found emission at the same velocity as the velocity of CH absorption found by Chaffee (1975). The clouds toward the Perseus OB2 association (e.g., Sargent 1979 and Federman 1980) and the Scorpius OB2 association (e.g., Bronfman 1980 and Meyers *et al.* 1982) show molecular radio emission and optical absorption at the same velocity. When a molecule is observed with both techniques, similar column densities are derived. We investigated further the association between diffuse clouds and dark clouds through observations of CH emission at 9 cm.

The CH radical is ideal for studying the association between the two kinds of clouds. Absorption at 4300 Å is seen along many lines of sight toward bright stars (Federman 1982). Theoretical models (Black and Dalgarno 1977; Black, Hartquist, and Dalgarno 1978; Federman and Glassgold 1980) indicate that the absorption arises from gas with densities between ~ 100 and $1000\ \mathrm{cm}^{-3}$. Emission from CH at 9 cm, which has been measured toward both bright stars (Lang and Willson 1978; Willson 1981) and dark clouds (e.g., Sandell *et al.* 1981), occurs in gas with similar densities. Other molecules, like CO, require larger densities for significant emission; though OH emission is possible at low densities, the detection of OH ultraviolet absorption is restricted to only a few directions.

We measured CH emission from the directions toward α Cam and κ Cas, as well as from dark clouds near these stars. Federman (1982) detected CH absorption toward the stars. The remainder of this report deals with our results for the two directions (§ II) and an analysis of the correspondence between diffuse clouds and dark clouds (§ III).

II. OBSERVATIONS

Measurements of the $F = 1\text{–}1$ Λ doublet of the ${}^2\Pi_{1/2}$, $J = \frac{1}{2}$ ground state of CH were made in 1981 July–August with the 43.5 m antenna of the National Radio Astronomy Observatory.[1] At the frequency of the $F = 1\text{–}1$ Λ transition (3335.481 MHz), the half-power beamwidth of the antenna is $\sim 9'$. Two 504-channel autocorrelators were operated in parallel with 1.25 MHz bandwidths and individual channel resolutions of 0.22 km s^{-1}. The spectra were obtained by frequency switching 0.625 MHz within the passband so that the line and its negative image would appear in the band. The spectra from both autocorrelators then were averaged, shifted, and smoothed with a boxcar function to yield an effective resolution of 0.66 km s^{-1}. When a line appeared in the spectra, a least-squares Gaussian fit was used to obtain

[1] The National Radio Astronomy Observatory is operated by Associated Universities for Research, Inc., under contract with the National Science Foundation.

the peak line intensity T_L, the full width at half-maximum ΔV, and the radial velocity in the local standard of rest V_{LSR}. If no line was present, an upper limit for T_L was calculated from twice the root mean square fluctuations about the baseline. Lastly, as a check on the day-to-day variation in T_L, the dark cloud L134 was observed; no variation in $T_L = 0.15$ K beyond the uncertainty in each measurement was seen.

The observational results are presented in Table 1, where the position of the source, T_L, ΔV, V_{LSR}, and the column density of CH are listed. The quoted errors are one standard deviation. For T_L, the root mean error in the baseline is used, while the errors for ΔV and V_{LSR} are from the least-squares Gaussian fit. The column density, N(CH), is calculated from the relation

$$N(\mathrm{CH}) \approx 2.9 \times 10^{14} \frac{T_x T_L \Delta V}{\eta_M(T_x \Omega_C/\Omega_M) - T_B} \mathrm{cm}^{-2} . \quad (1)$$

Here, T_x is the CH excitation temperature, and T_B the brightness temperature of the universal microwave background; η_M is the main beam efficiency; and Ω_C and Ω_M are the solid angles subtended by the cloud and by the main beam of the antenna. The values for these parameters were chosen in the following manner: from the measurements of CH in dark clouds by Rydbeck *et al.* (1976), T_x was set at -15 K; a value of 2.8 K was adopted for T_B; η_M was 0.60; and Ω_C and Ω_M were assumed to be equal. If the CH emission occurs under local thermodynamic equilibrium conditions such that $T_x \sim 40$–80 K, only slight changes ($\lesssim 20\%$) arise in the determination of N(CH). For comparison, ΔV, V_{LSR}, and N(CH) from the optical absorption measurements are shown in the notes to Table 1.

The results are displayed graphically in Figures 1–2 (Plates 15–16) and 3–4. The positions that were observed are indicated as overlays to the prints of the POSS plates in Figures 1 and 2. Figure 1 shows the sky near α Cam, while Figure 2 shows the sky surrounding κ Cas. Figures 3 and 4 present the spectra for the positions near α Cam and κ Cas. The velocity of the optical absorption from the diffuse cloud in front of the bright stars is shown as a vertical dashed line. The tick mark in the upper portion of Figures 3 and 4 indicates the uncertainty ($\pm 2\ \sigma$) in the determination of the velocity from the optical measurements.

For both areas of the sky, radio emission is found at the velocity of the optical absorption line of CH. Toward α Cam most, if not all, of the emission arises from the same parcel of gas sampled by the optical measurements. The value for N(CH) from the radio observations is somewhat larger than the value from the optical work, indicating that some of the emission may come from gas behind the stars. Within the uncertainties of each technique, the separate values agree. The radio data toward κ Cas are less conclusive because emission at the velocity

TABLE 1

OBSERVATIONAL RESULTS

Source	α(1950)	δ(1950)	T_L (K)	ΔV (km s^{-1})	V_{LSR} (km s^{-1})	N(CH)[a] (cm^{-2})
α Cam[b]	04^{h}49^{m}03^s.8	+66°15′40″	0.020 ± 0.003	1.42 ± 0.14	+0.57 ± 0.06	1.0(13)
α Cam A	04 17 03.7	+64 15 38	0.022 ± 0.006	1.69 ± 0.26	−12.21 ± 0.11	1.4(13)
			0.025 ± 0.006	1.67 ± 0.24	+0.23 ± 0.10	1.5(13)
			0.027 ± 0.006	3.42 ± 0.34	+4.24 ± 0.13	3.4(13)
α Cam B	04 32 33.7	+64 35 37	0.032 ± 0.006	2.95 ± 0.26	+3.14 ± 0.11	3.5(13)
α Cam C	04 40 03.9	+65 15 39	0.023 ± 0.004	3.17 ± 0.25	+0.55 ± 0.11	2.7(13)
α Cam D	04 53 03.8	+66 16 38	<0.008	(2.5)	...	<7.4(12)[c]
α Cam E	04 47 03.8	+65 45 38	0.012 ± 0.002	1.41 ± 0.19	−1.16 ± 0.08	6.2(12)
			0.009 ± 0.002	3.23 ± 0.37	+3.23 ± 0.15	1.1(13)
α Cam F	04 48 03.8	+66 55 37	<0.006	(2.5)	...	<5.5(12)[c]
α Cam G	04 52 03.8	+65 45 37	<0.010	(2.5)	...	<9.2(12)[c]
κ Cas[d]	00 30 08.6	+62 39 21	0.008 ± 0.002	3.85 ± 0.53	−19.15 ± 0.20	1.1(13)
			0.010 ± 0.002	1.55 ± 0.24	−15.62 ± 0.10	5.7(12)
			0.012 ± 0.002	2.06 ± 0.20	−12.04 ± 0.08	9.1(12)
			0.009 ± 0.002	5.05 ± 0.44	−4.37 ± 0.18	1.7(13)
κ Cas A	00 33 38.5	+63 09 51	0.030 ± 0.006	1.36 ± 0.18	−16.50 ± 0.08	1.5(13)
κ Cas B	00 40 08.5	+61 39 22	0.033 ± 0.005	1.24 ± 0.13	−12.34 ± 0.06	1.5(13)
κ Cas C	00 38 38.7	+62 39 21	0.046 ± 0.004	3.09 ± 0.14	−16.94 ± 0.06	5.2(13)
			0.021 ± 0.004	1.91 ± 0.23	−13.36 ± 0.10	1.5(13)
			0.021 ± 0.004	1.09 ± 0.15	−10.16 ± 0.06	8.4(12)
κ Cas D	00 42 38.5	+62 14 21	0.020 ± 0.004	3.26 ± 0.30	−18.02 ± 0.13	2.4(13)
			0.019 ± 0.004	2.76 ± 0.29	−12.00 ± 0.12	1.9(13)
κ Cas E	00 34 08.7	+61 29 22	0.018 ± 0.002	2.95 ± 0.16	−18.57 ± 0.07	2.0(13)

[a] Number in parentheses indicates power of 10.

[b] The optical results indicate: $\Delta V = 4.5 \pm 0.9$ km s^{-1}; $V_{LSR} = +1.3 \pm 0.8$ km s^{-1}; and N(CH) = 6.5(12) cm^{-2} (Federman 1982).

[c] In calculating upper limits to N(CH), a width of 2.5 km s^{-1} was assumed.

[d] The optical results indicate: $\Delta V = 3.5 \pm 0.6$ km s^{-1}; $V_{LSR} = -10.7 \pm 0.4$ km s^{-1}; N(CH) = 8.0(12) cm^{-2}; and a feature may exist at $V_{LSR} \sim -4.0$ km s^{-1} (Federman 1982).

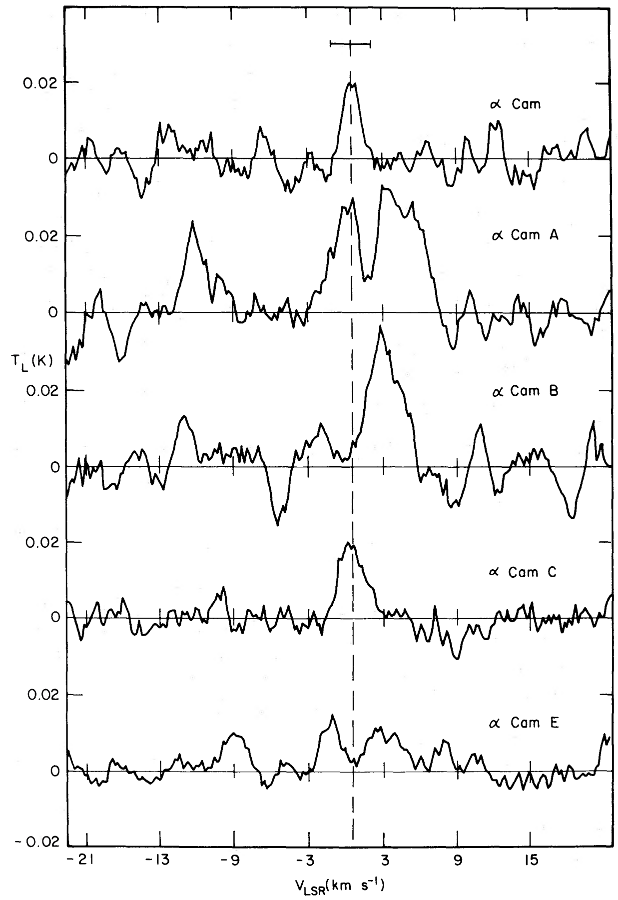

FIG. 3.—Spectra indicating detections of emission lines for directions toward α Cam and dark clouds near the star. The positions are shown in Fig. 1. The dashed line displays the velocity of CH absorption seen toward α Cam. The tick mark in the upper panel indicates the $\pm 2\ \sigma$ error associated with the velocity derived from the absorption measurements.

of absorption is not clearly present. A case for the emission can be made from optical work. Though the optical measurements of CH do not clearly show absorption at velocities other than at $V_{LSR} \sim -12$ km s^{-1}, atomic absorption is seen throughout the velocity range -20 to $+5$ km s^{-1} (Marschall and Hobbs 1972). The atomic absorption may indicate the presence of CH absorption below the limit of detection in the survey of Federman (1982). The derived value for N(CH) from the radio work is, however, consistent with the value obtained from the optical survey for $V_{LSR} \sim -12$ km s^{-1}.

Several dark clouds near each star also show radio emission at the velocity of optical CH absorption. The absorption toward α Cam probably is associated with the cloud α Cam C, where emission at no other velocity is apparent. Emission toward the dark cloud α Cam A is present at several velocities, including $V_{LSR} \sim 0$ km s^{-1}. The position α Cam E, which is between α Cam and α Cam C, also shows emission at the velocity of the absorption line. No dark clouds are located at the positions of α Cam D, α Cam F, and α Cam G; these positions were observed to set restrictions on the extent of the diffuse gas. The diffuse cloud in front of κ Cas is likely to be associated with the dark cloud κ Cas B. Emission at $V_{LSR} \sim -12$ km s^{-1} also is seen toward κ Cas C and κ Cas D, though emission at other velocities is present for these two directions. The present observations do not place strong restrictions on the extent of the diffuse cloud toward κ Cas because of (1) the limited number of measurements made of positions around the star and (2) the large value for the uncertainty in T_L toward κ Cas A.

Radio emission from the dark clouds is seen at velocities besides that seen from the diffuse cloud. Both stars are approximately 1 kpc from the Sun. The additional emission may come from gas behind the stars, but then dark clouds may be difficult to discern on POSS plates at distances larger than 1 kpc. Two explanations can be offered for the presence of only one velocity component seen in optical absorption toward the stars, while additional components are seen in radio emission in some of the dark clouds near the stars. First, both

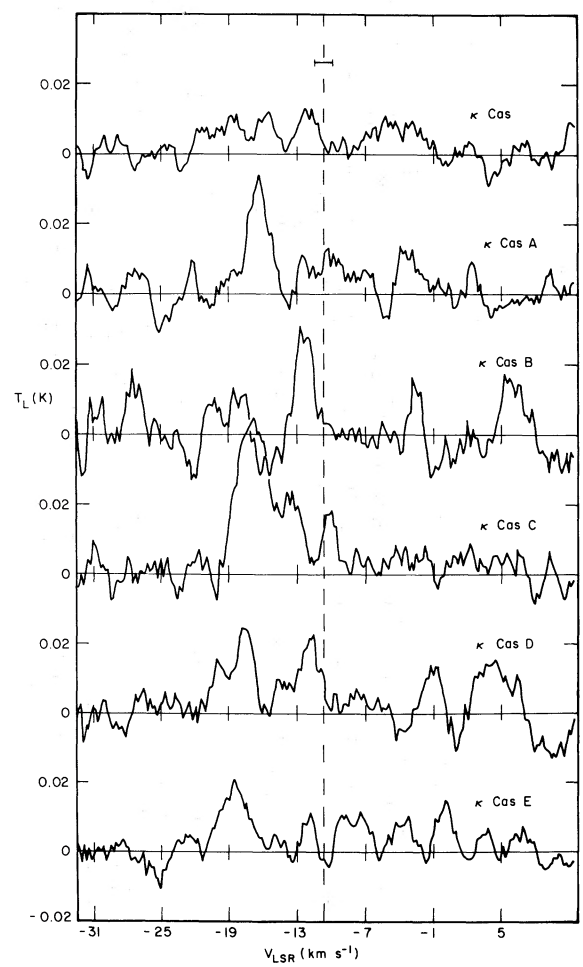

FIG. 4.—Spectra of areas near and toward κ Cas. The positions are indicated in Fig. 2. Otherwise, the description is similar to that for Fig. 3.

α Cam and κ Cas are supergiants; distances to supergiants are known to only a factor of 2. Thus the stars may be substantially closer than 1 kpc, eliminating the problem of discerning dark clouds at distances larger than 1 kpc. Second, all the clouds may be in front of the stars, but subtend different angles on the sky because the clouds vary in distance from the Sun and/or have different linear dimensions.

III. DISCUSSION

Optical surveys of CO (Federman *et al.* 1980) and of CH (Federman 1982) reveal that the molecular chemistry applicable to diffuse clouds can be extended to more opaque regions. For CH, the relationship between N(CH) and visual extinction A_V is similar for both diffuse and dark clouds. This fact is understandable in the terms of the equation for N(CH) derived from steady-state chemical models:

$$N(\mathrm{CH}) = \left[\frac{k_1 n(\mathrm{C}^+)}{G(\mathrm{CH}) + k_2 n(\mathrm{C}^+)}\right] N(\mathrm{H}_2)\ \mathrm{cm}^{-2}\ . \quad (2)$$

The rate constants k_1 and k_2 are for the radiative association reaction, $\mathrm{C}^+ + \mathrm{H}_2 \rightarrow \mathrm{CH}_2{}^+ + h\nu$, and the ion-molecule reaction, $\mathrm{C}^+ + \mathrm{CH} \rightarrow \mathrm{C}_2{}^+ + \mathrm{H}$. The photodestruction rate for CH is G(CH). Since 9 cm emission arises from low density gas, C^+ is the progenitor ion for the formation of CH in both diffuse and dark clouds. The ratio $N(\mathrm{H}_2)/A_V$ does not vary appreciably for clouds with extinctions less than or equal to 4 mag. The main difference between the CH chemistry for diffuse clouds and dark clouds is in the relative contributions of the two destruction terms that are in the denominator of equation (2). Because the CH chemistry for both kinds of clouds is based on the same rate equation, as indicated by the observations, Federman (1982) proposed that diffuse clouds containing molecules are the outer regions of dark clouds.

The above hypothesis is confirmed by the present observations. The optical absorption and radio emission of CH occur at the same velocity toward the two stars studied here, and the two observational techniques yield similar column densities for CH. Most importantly, a dark cloud near each star shows emission only at the velocity of the cloud in front of the star. The value for N(CH) for each dark cloud is significantly larger (factor of ~ 2) than the value for N(CH) in front of the star. Furthermore, the visual extinction is greater toward the dark cloud. The diffuse cloud toward each of the two stars, therefore, appears to be an outer region of the dark cloud near the two stars.

The scope of this conclusion can be enlarged further. Federman (1981) argued that the neutral atomic data from diffuse clouds indicated a layered cloud. Below a threshold in column density for neutral atomic species, these species are associated with atomic gas. Above the threshold $[N(\mathrm{H}_2) \gtrsim 10^{19}\ \mathrm{cm}^{-2}]$, the species are associated with molecular gas, which is enveloped by the atomic gas. The picture that emerges is one where an interstellar cloud has an opaque, molecular core, surrounded by a transparent molecular layer, and has an outer envelope of atomic gas.

We propose that most diffuse clouds seen in optical observations with $N(\mathrm{H\ I}) \gtrsim 10^{20}\ \mathrm{cm}^{-2}$ are associated with dark clouds. Most of the clouds studied with the *Copernicus* satellite have column densities for atomic hydrogen above $10^{20}\ \mathrm{cm}^{-2}$. Likewise, most optical measurements for directions with an unknown amount of atomic hydrogen probably sample gas conforming to the limit on N(H I) because the amount of extinction ($A_V \gtrsim 0.02$ mag) from the gas indicates a sufficient number of hydrogen atoms (cf. Bohlin, Savage, and Drake 1978). Thus, a layered interstellar cloud, as presented above, is commonplace, and future analyses of interstellar clouds should take this view into account.

We would like to thank N. Evans for his constructive comments regarding the manuscript. This work was supported by grant F-623 from the Robert A. Welch Foundation (S. R. F.).

REFERENCES

Black, J. H., and Dalgarno, A. 1977, *Ap. J. Suppl.*, **34**, 405.
Black, J. H., Hartquist, T. W., and Dalgarno, A. 1978, *Ap. J.*, **224**, 448.
Bohlin, R. C., Savage, B. D., and Drake, J. F. 1978, *Ap. J.*, **224**, 132.
Bronfman, L. 1980, M.S. thesis, Universidad de Chile.
Chaffee, F. H. 1975, *Ap. J.*, **199**, 379.
Crutcher, R. M. 1979, *Ap. J.* (*Letters*), **231**, L151.
Federman, S. R. 1980, *Ap. J.* (*Letters*), **241**, L109.
———. 1981, *Astr. Ap.*, **96**, 198.
———. 1982, *Ap. J.*, **257**, 125.
Federman, S. R., and Glassgold, A. E. 1980, *Astr. Ap.*, **89**, 113.
Federman, S. R., Glassgold, A. E., Jenkins, E. B., and Shaya, E. J. 1980, *Ap. J.*, **242**, 545.
Lang, K. R., and Willson, R. F. 1978, *Ap. J.*, **224**, 125.
Liszt, H. S. 1979, *Ap. J.* (*Letters*), **233**, L147.
Marschall, L. A., and Hobbs, L. M. 1972, *Ap. J.*, **173**, 43.
Meyers, K. A., Snow, T. P., Federman, S. R., and Breger, M. 1982, *Ap. J.*, submitted.
Rydbeck, O. E. H., Kollberg, E., Hjalmarson, A., Sume, A., Elder, J., and Irvine, W. M. 1976, *Ap. J. Suppl.*, **31**, 333.
Sandell, G., Johansson, L. E. B., Nguyen-Q-Rieu, and Matilla, K. 1981, *Astr. Ap.*, **97**, 317.
Sargent, A. I. 1979, *Ap. J.*, **233**, 163.
Willson, R. F. 1981, *Ap. J.*, **247**, 116.

S. R. FEDERMAN: Department of Astronomy, University of Texas, Austin, TX 78712

R. F. WILLSON: Department of Physics, Tufts University, Medford, MA 02155

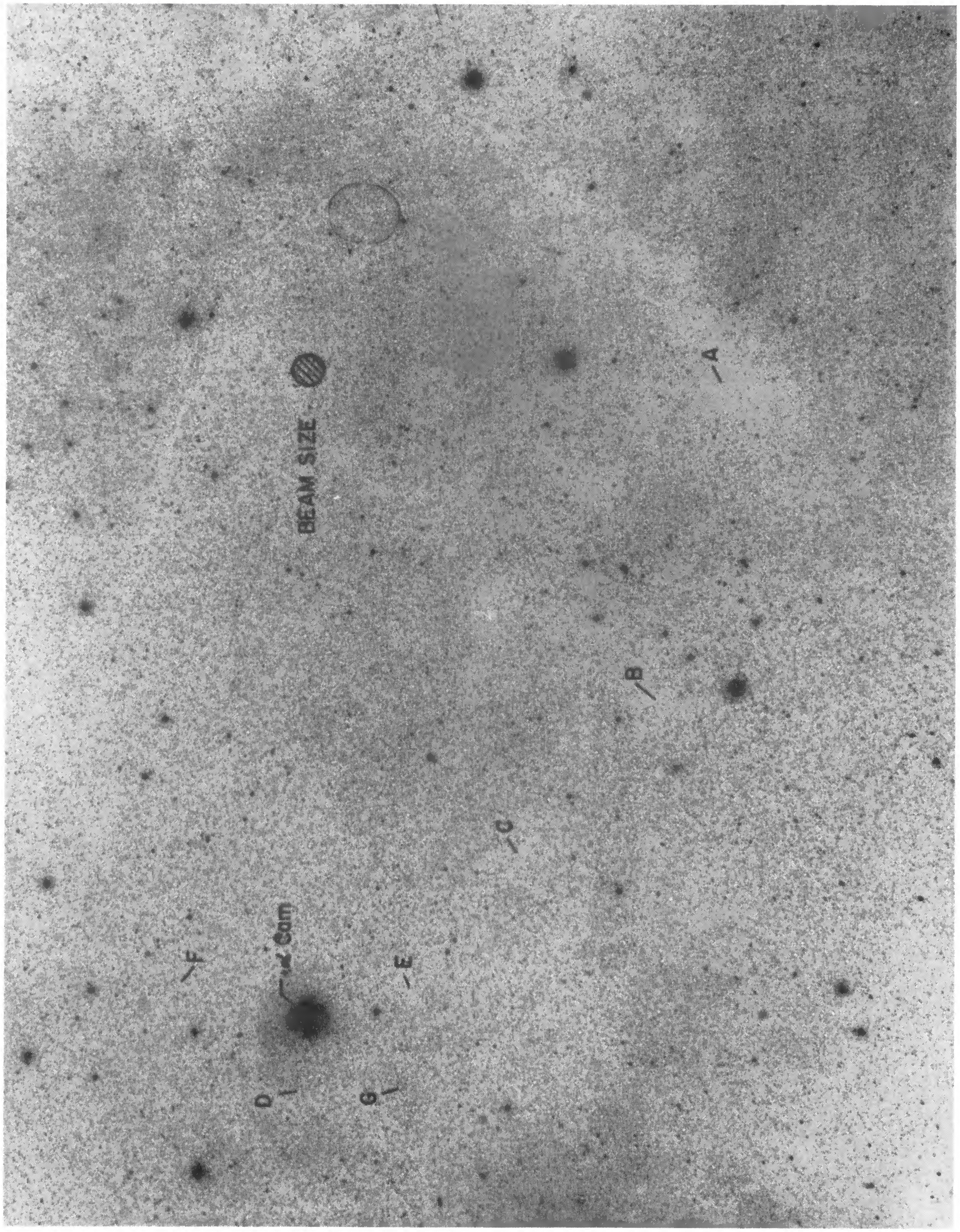

FIG. 1.—Print of the POSS plate for the sky surrounding α Cam. The positions studied are indicated.

FEDERMAN AND WILLSON (*see* page 125)

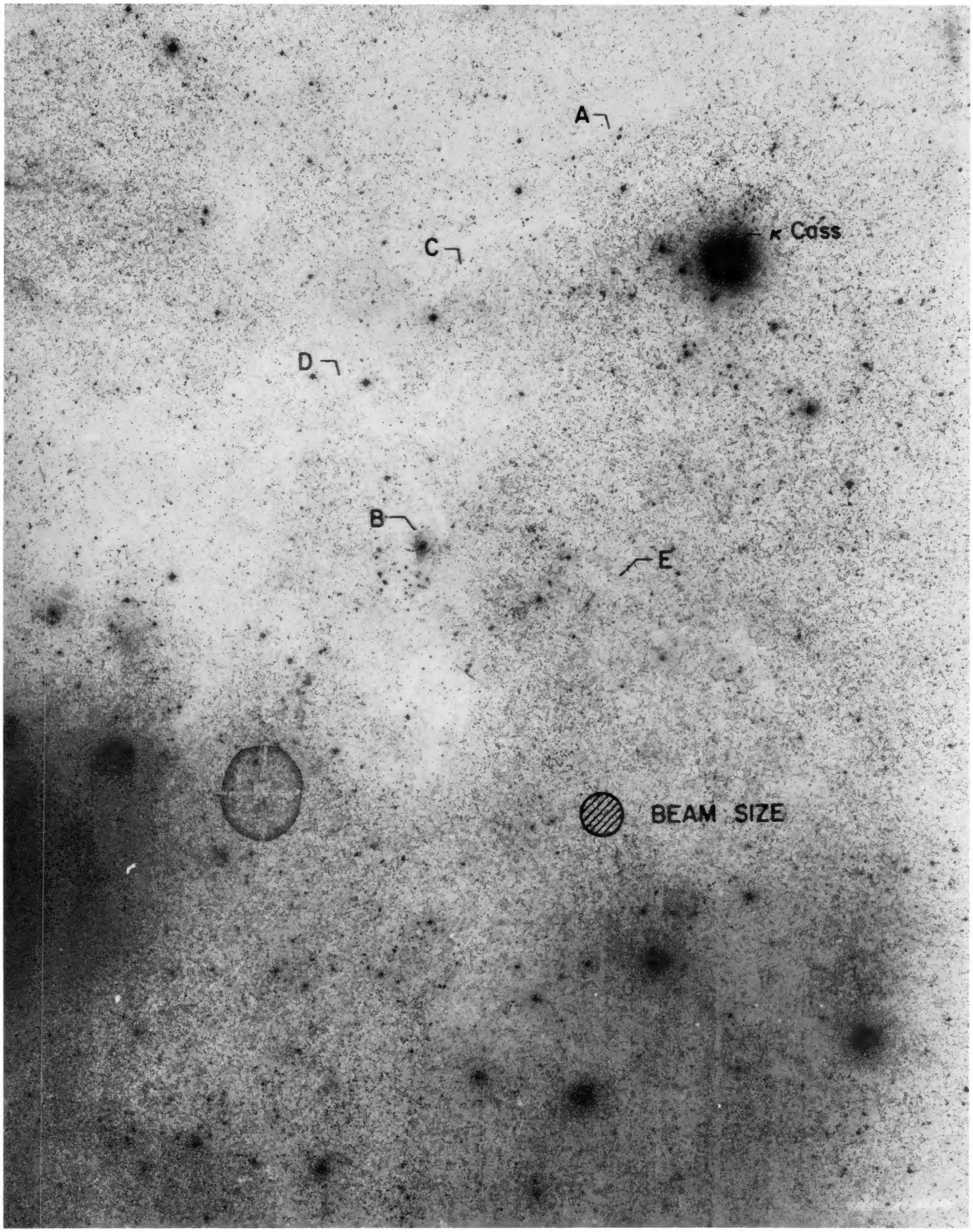

FIG. 2.—Same as Fig. 1 for the sky surrounding κ Cas.

FEDERMAN AND WILLSON (*see* page 125)